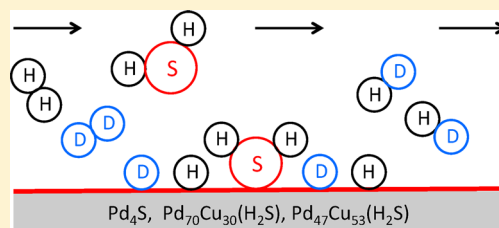


H₂-D₂ Exchange Kinetics in the Presence of H₂S over Pd₄S, Pd₇₀Cu₃₀, and Pd₄₇Cu₅₃ Surfaces

Casey P. O'Brien,^{†,‡} James B. Miller,^{*,†,‡} Bryan D. Morreale,[†] and Andrew J. Gellman^{†,‡}[†]National Energy Technology Laboratory-Regional University Alliance (NETL-RUA), U.S. Department of Energy, Pittsburgh, Pennsylvania 15236, United States[‡]Department of Chemical Engineering, Carnegie Mellon University, Pittsburgh, Pennsylvania 15213, United States

ABSTRACT: H₂S retards H₂ transport across Pd membranes used for H₂ separation by forming a Pd₄S scale that has both low H₂ dissociation activity and low H-atom permeability. As hydrogen purification membranes, alloys such as Pd₇₀Cu₃₀ and Pd₄₇Cu₅₃ are attractive alternatives to pure Pd due to their resistance to formation of bulk sulfides. Nonetheless, exposure to H₂S can decrease the permeability of Pd₇₀Cu₃₀ and Pd₄₇Cu₅₃ membranes, presumably by poisoning the catalytic activity of their surfaces for H₂ dissociation. In this work, the effect of H₂S on H₂ dissociation on Pd₄S, Pd₇₀Cu₃₀, and Pd₄₇Cu₅₃ surfaces is investigated by microkinetic analysis of H₂-D₂ exchange kinetics over Pd₄S, Pd₇₀Cu₃₀, and Pd₄₇Cu₅₃ surfaces in the presence of varying concentrations of H₂S at near-ambient H₂+D₂ pressure. We show that the rate of H₂-D₂ exchange over all three surfaces is significantly suppressed when H₂S is added to H₂/D₂/Ar reactant mixtures and that the suppression of H₂-D₂ exchange increases with increasing H₂S concentration. Microkinetic analysis of the H₂-D₂ exchange kinetics reveals that H₂S decreases the rate of H₂-D₂ exchange by two distinct mechanisms: (1) increasing the intrinsic barrier to H₂ dissociation and (2) blocking H₂ dissociation sites.



1. INTRODUCTION

Coal gasification has the potential to produce affordable supplies of H₂, liquid fuels, and electricity with near-zero greenhouse gas emissions.¹ Separation of gasification products, for both recovery of H₂ and capture of CO₂, is an important unit operation in all advanced gasification processes. Dense Pd-based membranes have been developed for this application because of their ability to separate very high purity H₂ from “clean” mixed gases at economical rates;^{2–5} however, ppm-levels of H₂S in the coal derived gas feed greatly reduce the rate of H₂ transport across Pd-based membranes.^{6–14}

Pd membranes can separate high purity H₂ from H₂/CO₂ gas mixtures because of the unique way in which H₂ interacts with the membrane: molecular H₂ adsorbs dissociatively on the Pd surface, producing H atoms which penetrate the surface and then diffuse through the bulk of the Pd lattice and finally desorb as H₂ by recombination at the opposite surface. Only H atoms permeate through the Pd lattice a significant rate, resulting in near-infinite selectivity for H₂ separation.^{5,15,16} In the absence of surface poisons, such as H₂S, H₂ dissociates spontaneously on the Pd surface^{17–19} and atomic H permeates rapidly through the Pd lattice.^{5,20} However, H₂S severely retards H₂ permeation across Pd membranes by reacting to form a bulk Pd-sulfide (Pd₄S) scale that is much less active for H₂ dissociation than Pd and is about an order-of-magnitude less permeable to H than Pd.^{10,12–14}

PdCu alloy membranes are attractive alternatives to pure Pd membranes because of their tolerance, relative to Pd, to sulfur-compounds at high temperatures.^{9–11} Pd₇₀Cu₃₀ (atom %) and Pd₄₇Cu₅₃ are two specific compositions that have received

significant attention.^{7,8,10,11,14,21–24} These alloys are more resistant to bulk sulfidation than Pd^{7,10,14} and H transport through them is not significantly affected by 1000 ppm H₂S in the gas at temperatures above ~900 K.^{10,11,25} At lower temperatures (~600 K), however, 1000 ppm H₂S blocks hydrogen transport through Pd₇₀Cu₃₀ and Pd₄₇Cu₅₃ alloys almost completely.¹⁰ While Pd₇₀Cu₃₀ and Pd₄₇Cu₅₃ do not form thick sulfide scales at low temperatures, thin (1–5 μm) sulfide layers have been observed on their surfaces. It has been suggested that these thin layers poison the catalytic activity of their parent surfaces for H₂ dissociation.¹⁰ However, there is little direct experimental evidence to support this hypothesis.

In this work, the effect of H₂S on the rate of H₂ dissociation on Pd₄S, Pd₇₀Cu₃₀, and Pd₄₇Cu₅₃ foil surfaces is investigated by microkinetic analysis of H₂-D₂ exchange reaction kinetics measured in the presence of H₂S at near ambient pressure. We show that the rate of H₂ dissociation over all three surfaces is significantly reduced by adding 100 ppm H₂S to the H₂/D₂/Ar feed gas, relative to that on the clean Pd, Pd₇₀Cu₃₀, and Pd₄₇Cu₅₃ surfaces in the absence of H₂S, and the rate of H₂ dissociation decreases as the H₂S concentration is increased up to 2000 ppm. H₂S decreases the rate of H₂ dissociation on all three surfaces both by blocking H₂ dissociation sites and by increasing the barrier to H₂ dissociation relative to that on the clean Pd, Pd₇₀Cu₃₀, and Pd₄₇Cu₅₃ surfaces in the absence of H₂S.

Received: May 23, 2012

Revised: July 23, 2012

Published: August 14, 2012

2. EXPERIMENTAL SECTION

The experimental apparatus for the H₂-D₂ exchange experiments has been described in detail elsewhere.¹⁸ Briefly, H₂S, H₂, D₂, and Ar were fed to a quartz tube reactor (4 mm ID) that was packed with diced Pd foil (Alfa Aesar, 25 μm thick, 99.9% metals purity), Pd₇₀Cu₃₀ foil (ACI Alloys, Inc., 100 μm thick, 99.0% metals purity), or Pd₄₇Cu₅₃ foil (ATI Wah Chang, 25 μm thick, 99.0% metals purity). The total surface area of the foil catalysts used in all experiments was ~19 cm². The product gas stream was analyzed by mass spectrometry (Stanford Research Systems, RGA 200) to determine the HD concentrations and thus, the H₂/D₂ conversion. The quartz tube reactor was heated in a tube furnace (Barnstead/ThermoLyne 211000). We used four different H₂S concentrations in the H₂/D₂/Ar feed gas: 100, 200, 1000, and 2000 ppm. The target concentration of H₂S in the feed gas mixture was achieved by diluting either a (1.09 ± 0.02%) H₂S/H₂ gas mixture (Matheson Tri-Gas) or a (0.107 ± 0.002%) H₂S/H₂ gas mixture (Matheson Tri-Gas) with pure H₂ (99.999% purity, Valley National Gases). The 0.107% H₂S/H₂ gas mixture was used for H₂S concentrations of 100 and 200 ppm and the 1.09% H₂S/H₂ gas mixture was used for H₂S concentrations of 1000 and 2000 ppm. To measure the H₂-D₂ exchange kinetics over a range of flow rates and H₂/D₂ partial pressures, three different H₂/D₂/Ar feed gas combinations were used for each H₂S concentration: 9 mL/min of both H₂ and D₂ (9H₂/9D₂), 4.5 mL/min of both H₂ and D₂ (4.5H₂/4.5D₂), and 4.5 mL/min of both H₂ and D₂ diluted with 9 mL/min of Ar (9Ar/4.5H₂/4.5D₂). The flow rates of the feed gases were regulated with mass flow controllers (Aalborg GFC 17). The total pressure in the reactor was measured with a Baratron pressure gauge. Table 1 lists the H₂S concentrations, flow rates, and total pressures for the 12 different feed gas conditions used in the H₂-D₂ exchange experiments.

The Pd₄S catalyst was initially prepared in the H₂-D₂ exchange reactor by flowing a 1.09% H₂S/H₂ gas mixture over a pure Pd foil (Alfa Aesar, 25 μm thick, 99.9% metals purity) catalyst bed for ~40 h at 773 K. On the basis of the kinetics of Pd sulfidation,¹⁰ this treatment was sufficient to completely sulfide the 25-μm-thick Pd foil to Pd₄S. Because thick sulfides are not expected to form on the Pd₇₀Cu₃₀ and Pd₄₇Cu₅₃ foil catalysts under the conditions of the H₂-D₂ exchange experiments,¹⁰ the Pd₇₀Cu₃₀ and Pd₄₇Cu₅₃ foil catalysts were not pretreated in a similar manner. Prior to the H₂-D₂ exchange experiments, the Pd₄S, Pd₇₀Cu₃₀, and Pd₄₇Cu₅₃ foil catalyst beds were heated to ~1000 K in a 1000 ppm H₂S in H₂ gas mixture and held at that temperature overnight. After the initial heat treatment, the H₂S/H₂/D₂/Ar feed gas mixture was introduced to the reactor and the product gas composition was analyzed by the mass spectrometer. Steady-state mass spectrometer signals were collected at constant temperature and the temperature was decreased from 1000 K in a stepwise fashion until the H₂-D₂ exchange rate was negligible.

3. KINETIC MODEL

We derived the H₂-D₂ exchange model based on four assumptions:

- (1) The H₂-D₂ exchange reaction can be modeled using Langmuir–Hinshelwood kinetics by considering only dissociative adsorption and recombinative desorption of H₂, D₂, and HD; and nondissociative adsorption of H₂S. H₂S, adsorbed H and adsorbed D compete for

Table 1. Feed Gas Flow Rates for the 12 Different Feed Gas Conditions Used in H₂-D₂ Exchange Experiments in the Presence of H₂S

feed gas condition	H ₂ S concentration (ppm)	feed gas flow rates (mL/min)				P _{total} (kPa)	
		1% H ₂ S/H ₂	0.1% H ₂ S/H ₂	H ₂	D ₂		Ar
4.5H ₂ /4.5D ₂	2000 ± 200	1.65	0	2.86	4.5	0	104
4.5H ₂ /4.5D ₂	1000 ± 200	0.83	0	3.68	4.5	0	104
4.5H ₂ /4.5D ₂	200 ± 20	0	1.68	2.82	4.5	0	104
4.5H ₂ /4.5D ₂	100 ± 20	0	0.84	3.66	4.5	0	104
9H ₂ /9D ₂	2000 ± 100	3.31	0	5.73	9	0	107
9H ₂ /9D ₂	1000 ± 100	1.65	0	7.36	9	0	107
9H ₂ /9D ₂	200 ± 10	0	3.37	5.63	9	0	107
9H ₂ /9D ₂	100 ± 10	0	1.69	7.31	9	0	107
9Ar/4.5H ₂ /4.5D ₂	2000 ± 100	3.31	0	1.23	4.5	9	111
9Ar/4.5H ₂ /4.5D ₂	1000 ± 100	1.65	0	2.86	4.5	9	111
9Ar/4.5H ₂ /4.5D ₂	200 ± 10	0	3.37	1.13	4.5	9	111
9Ar/4.5H ₂ /4.5D ₂	100 ± 10	0	1.68	2.82	4.5	9	111

adsorption sites. We observed evidence of H₂S dissociation: H₂-D₂ exchange in the presence of H₂S produced small, but detectable, quantities of HDS and D₂S on all three surfaces. However, more complex models that included dissociation of H₂S to SH and S did not fit the data significantly better than the simple nondissociative adsorption model.

- (2) Adsorbed H₂S is in equilibrium with gas-phase H₂S.
- (3) Kinetic isotopic effects can be ignored.
- (4) All the parameters in our model (i.e., activation barriers and pre-exponents) are independent of coverage and temperature, and constant for each surface composition.

Following these assumptions, we derived the H₂-D₂ exchange model by substituting the microkinetic expression for the rate of HD production into a mole balance on HD. A detailed derivation of the kinetic model is given in the Appendix. With this model the flow rate of HD exiting the reactor ($F_{\text{HD,out}}$) is given by the expression:

$$F_{\text{HD,out}} = F_{\text{H}_2,\text{feed}} \left[1 - \exp \left\{ \left(-k_{\text{ads}} P_{\text{total}} A \right) / \left(F_{\text{total}} \left(1 + K_{\text{H}_2\text{S}} P_{\text{H}_2\text{S}} + \sqrt{2 \frac{k_{\text{ads}}}{k_{\text{des}}} P_{\text{H}_2,\text{feed}}} \right)^2 \right) \right\} \right] \quad (1)$$

where $F_{\text{H}_2,\text{feed}}$ is the flow rate of H₂ in the feed gas, k_{ads} is the H₂ adsorption rate constant, P_{total} is the total pressure in the reactor, A is the catalyst surface area, F_{total} is the total gas flow rate through the reactor, k_{des} is the H₂ desorption rate constant, $P_{\text{H}_2,\text{feed}}$ is the partial pressure of H₂ in the feed gas (equal to $P_{\text{D}_2,\text{feed}}$), $P_{\text{H}_2\text{S}}$ is the partial pressure of H₂S in the feed gas, and

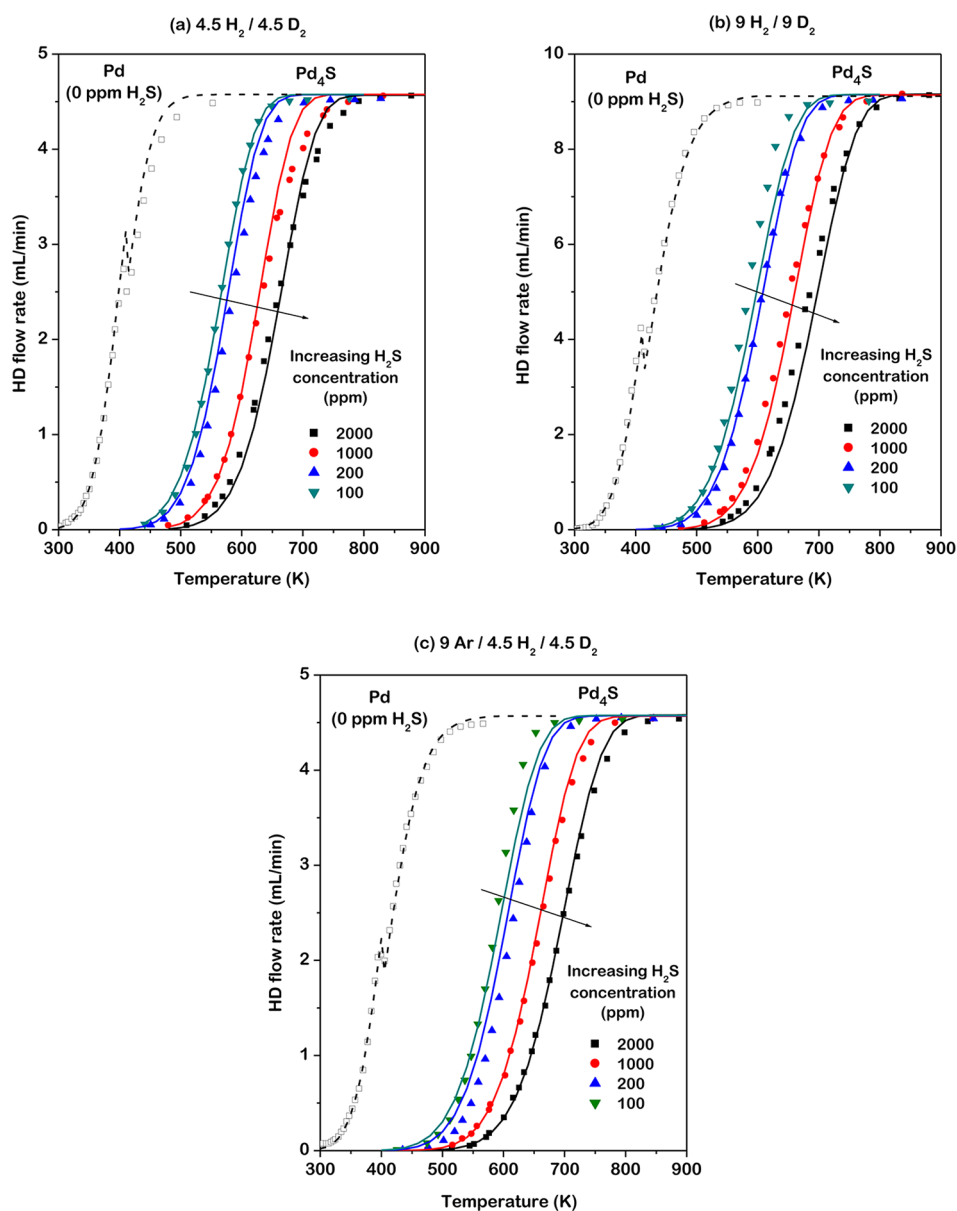


Figure 1. HD flow rates exiting a Pd foil catalyst bed without H₂S in the feed gas (Pd (0 ppm H₂S)), and a Pd₄S catalyst bed with H₂S concentrations of 100, 200, 1000, and 2000 ppm in the feed gas. The solid lines are fits of the microkinetic model for H₂-D₂ exchange to the data. The feed gas streams are (a) 4.5 mL/min each of H₂ and D₂, (b) 9 mL/min each of H₂ and D₂, and (c) 9 mL/min of Ar with 4.5 mL/min each of H₂ and D₂. The Pd₄S catalyst with H₂S in the feed gas is much less active for H₂-D₂ exchange than the pure Pd catalyst bed without H₂S in the feed gas and the activity of Pd₄S decreases with increasing H₂S concentration.

$K_{\text{H}_2\text{S}}$ is the H₂S adsorption equilibrium constant. The H₂ adsorption rate constant, k_{ads} , and the H₂ desorption rate constant, k_{des} , have Arrhenius forms:

$$k_{\text{ads}} = \nu_{\text{ads}} \exp\left(\frac{-\Delta E_{\text{ads}}^\ddagger}{k_{\text{B}}T}\right) \quad (2a)$$

$$k_{\text{des}} = \nu_{\text{des}} \exp\left(\frac{-\Delta E_{\text{des}}^\ddagger}{k_{\text{B}}T}\right) \quad (2b)$$

where ν_{ads} is the H₂ adsorption pre-exponent, $\Delta E_{\text{ads}}^\ddagger$ is the H₂ dissociative adsorption activation barrier, ν_{des} is the H₂ desorption pre-exponent, $\Delta E_{\text{des}}^\ddagger$ is the H₂ recombinative desorption activation barrier, and k_{B} is the Boltzmann constant. The H₂S equilibrium constant has the form:

$$K_{\text{H}_2\text{S}} = \exp\left(\frac{\Delta S_{\text{H}_2\text{S}}}{k_{\text{B}}}\right) \exp\left(\frac{-\Delta H_{\text{H}_2\text{S}}}{k_{\text{B}}T}\right) \quad (3)$$

where $\Delta S_{\text{H}_2\text{S}}$ is the entropy of H₂S adsorption and $\Delta H_{\text{H}_2\text{S}}$ is the enthalpy of H₂S adsorption. The coverage of H₂S ($\theta_{\text{H}_2\text{S}}$) during H₂-D₂ exchange is given by

$$\theta_{\text{H}_2\text{S}} = \frac{K_{\text{H}_2\text{S}}P_{\text{H}_2\text{S}}}{1 + K_{\text{H}_2\text{S}}P_{\text{H}_2\text{S}} + \sqrt{2\frac{k_{\text{ads}}}{k_{\text{des}}}P_{\text{H}_2,\text{feed}}}} \quad (4)$$

To determine the values of ν_{ads} , $\Delta E_{\text{ads}}^\ddagger$, ν_{des} , $\Delta E_{\text{des}}^\ddagger$, $\Delta S_{\text{H}_2\text{S}}$, and $\Delta H_{\text{H}_2\text{S}}$ that describe H₂-D₂ exchange over each catalyst, a numerical solver was used to find the values of $\log(\nu_{\text{ads}})$, $\Delta E_{\text{ads}}^\ddagger$, $\log(\nu_{\text{des}})$, $\Delta E_{\text{des}}^\ddagger$, $\Delta S_{\text{H}_2\text{S}}$, and $\Delta H_{\text{H}_2\text{S}}$ that minimize the error between the measured HD product flow rates and the flow

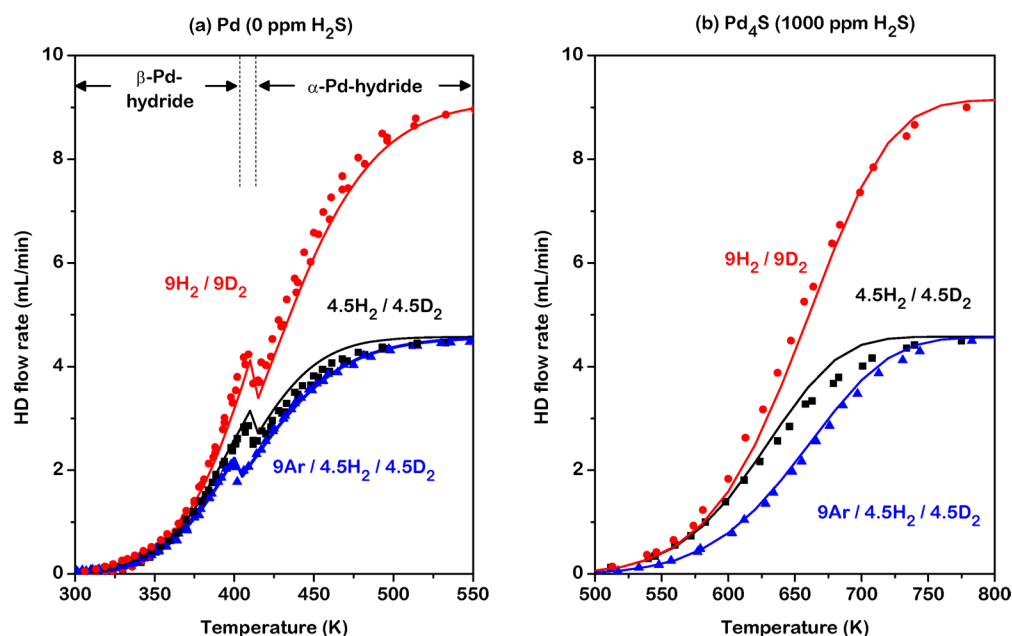


Figure 2. HD flow rates exiting the (a) Pd foil catalyst bed and the (b) Pd₄S catalyst bed with 1000 ppm H₂S in the feed gas, each with three different H₂/D₂/Ar feed gas combinations: 9 mL/min each of H₂ and D₂ (9H₂/9D₂), 4.5 mL/min each of H₂ and D₂ (4.5H₂/4.5D₂), and 4.5 mL/min each of H₂ and D₂ diluted with 9 mL/min of Ar (9Ar/4.5H₂/4.5D₂). The solid lines are fits of the microkinetic model for H₂-D₂ exchange to the data. Diluting the 4.5H₂/4.5D₂ feed gas with Ar (9Ar/4.5H₂/4.5D₂) does not significantly reduce the HD flow rate exiting the pure Pd foil catalyst bed, indicating desorption-limited H₂-D₂ exchange. In contrast, the HD flow rate exiting the Pd₄S catalyst bed in the presence of 1000 ppm H₂S is significantly reduced by diluting the H₂/D₂ feed gas with Ar, indicating that H₂ adsorption on Pd₄S is rate-limiting.

rates predicted by the model at all temperatures, reactant flow rates, and H₂ partial pressures. For each catalyst, the minimization was performed over 160 (Pd₄₇Cu₅₃(H₂S)) to 260 (Pd₄S) data points. The uncertainty in these solver-optimized parameters was estimated with a “SolverAid” program.²⁶

The model is based on one that we successfully used to describe H₂-D₂ exchange over Pd, Cu, and alloy catalysts in the absence of H₂S.¹⁸ We reported that values of $\Delta E_{\text{ads}}^{\ddagger}$ and $\Delta E_{\text{des}}^{\ddagger}$ extracted by fitting the original model to exchange data acquired over clean Pd and Cu catalysts compared well with values published by other researchers, thereby validating the original model. The model we use in this report differs from the original model only by addition of the $K_{\text{H}_2\text{S}}$ term to describe the coverage of H₂S (eqs 1 and 3).

4. RESULTS AND DISCUSSION

4.1. H₂-D₂ Exchange over Pd₄S in the Presence of H₂S.

The effect of H₂S on H₂ dissociative adsorption on Pd₄S was investigated by measurement of the H₂-D₂ exchange kinetics over a fixed bed of Pd₄S in the presence of H₂S. A description of the procedure for preparing the Pd₄S sample from Pd foil is given in the Experimental Section. H₂-D₂ exchange was carried out by feeding a H₂S/H₂/D₂/Ar gas mixture to the Pd₄S catalyst bed over a range of temperatures, while the product gas composition was analyzed with a mass spectrometer. Four different feed gas H₂S concentrations (100, 200, 1000, and 2000 ppm) were used, each with three different H₂, D₂, and Ar feed gas flow rates for a total of 12 different feed gas conditions. Figure 1 shows the HD flow rates exiting the Pd₄S catalyst bed with 100, 200, 1000, and 2000 ppm H₂S in the feed gas, and with (a) 4.5 mL/min of H₂ and D₂ in the feed gas, (b) 9 mL/min of H₂ and D₂ in the feed gas, and (c) 4.5 mL/min of H₂ and D₂ diluted with 9 mL/min of Ar in the feed gas. Previously

reported HD flow rates exiting a pure Pd foil catalyst bed without H₂S in the feed gas are shown in Figure 1 for comparison.¹⁸ Under all conditions, the HD conversion goes from 0 to 100%. Clearly the temperatures ranges over which this occurs increase with increasing $P_{\text{H}_2\text{S}}$, indicating that the presence of H₂S in the gas phase severely retards H₂-D₂ exchange. For all three H₂/D₂/Ar feed gas combinations, the onset of H₂-D₂ exchange occurs at ~300 K on the clean Pd catalyst in the absence of H₂S, whereas the onset of H₂-D₂ exchange occurs at ~450 K on the Pd₄S catalyst with 100 ppm H₂S in the feed gas. Increasing the H₂S concentration in the feed gas from 100 ppm to 2000 ppm results in further decreases in the rate of H₂-D₂ exchange over Pd₄S. The solid curves are fits of the microkinetic model to the data, which we will return to later in this section.

Figure 2 displays a subset of the data from Figure 1 in a manner that highlights the effects of the different H₂, D₂, and Ar flow rates on the reaction rates. Figure 2a shows the HD flow rate exiting a pure Pd foil catalyst bed with 0 ppm H₂S in the feed gas and 9 mL/min of H₂ and D₂ (9H₂/9D₂), 4.5 mL/min each of H₂ and D₂ (4.5H₂/4.5D₂), and 4.5 mL/min each of H₂ and D₂ diluted with 9 mL/min of Ar (9Ar/4.5H₂/4.5D₂). The discontinuity in the HD flow rate exiting the Pd (0 ppm H₂S) catalyst bed at ~400 K reflects an activity change related to the β -Pd-hydride to α -Pd-hydride phase transition.¹⁸ Over the clean Pd surface in the absence of H₂S, reducing the H₂ and D₂ partial pressures (P_{H_2}) by diluting the feed gas with Ar did not significantly reduce HD production (compare blue triangles and black squares in Figure 2a). As we reported previously,¹⁸ this response is characteristic of H₂-D₂ exchange in which *recombinative desorption* is the rate limiting step. Figure 2b shows the HD flow rates exiting the Pd₄S catalyst bed at the same feed gas rates but with 1000 ppm H₂S in the gas stream. In this case (and at other H₂S concentrations, not shown in

Table 2. Adsorption Pre-Exponents (ν_{ads}), Adsorption Barriers ($\Delta E_{\text{ads}}^\ddagger$), Desorption Pre-Exponents (ν_{des}), Desorption Barriers ($\Delta E_{\text{des}}^\ddagger$), Enthalpy Change for H₂S Adsorption ($\Delta H_{\text{H}_2\text{S}}$), and Entropy Change for H₂S Adsorption ($\Delta S_{\text{H}_2\text{S}}$), on β -Pd-hydride, α -Pd-hydride, Pd₄S in the Presence of H₂S, Pd₇₀Cu₃₀, Pd₇₀Cu₃₀ in the Presence of H₂S, B2 Pd₄₇Cu₅₃, and Pd₄₇Cu₅₃ in the Presence of H₂S

	ν_{ads} (mol/m ² /s/Pa)	$\Delta E_{\text{ads}}^\ddagger$ (eV)	ν_{des} (mol/m ² /s)	$\Delta E_{\text{des}}^\ddagger$ (eV)	$\Delta S_{\text{H}_2\text{S}}$ (eV/K)	$\Delta H_{\text{H}_2\text{S}}$ (eV)
β -Pd-hydride ¹⁸	$10^{-3.7 \pm 0.7}$	0.3 ± 0.1	$10^{5.8 \pm 0.4}$	0.63 ± 0.03		
α -Pd-hydride ¹⁸	$10^{-5.4 \pm 0.4}$	0.12 ± 0.04	$10^{6.3 \pm 0.8}$	0.68 ± 0.06		
Pd ₄ S (H ₂ S)	$10^{-2.3 \pm 0.3}$	0.58 ± 0.03	<i>a</i>	<i>a</i>	$-10^{-3.14 \pm 0.03}$	-0.21 ± 0.03
Pd ₇₀ Cu ₃₀ ¹⁸	$10^{-5.6 \pm 0.2}$	0.09 ± 0.02	$10^{5.7 \pm 0.3}$	0.52 ± 0.02		
Pd ₇₀ Cu ₃₀ (H ₂ S)	$10^{-0.7 \pm 0.5}$	0.84 ± 0.06	<i>a</i>	<i>a</i>	$-10^{-3.15 \pm 0.05}$	-0.21 ± 0.05
B2 Pd ₄₇ Cu ₅₃ ¹⁸	$10^{-5.2 \pm 0.2}$	0.15 ± 0.02	$10^{7.4 \pm 0.5}$	0.67 ± 0.03		
Pd ₄₇ Cu ₅₃ (H ₂ S)	$10^{-3.6 \pm 0.4}$	0.46 ± 0.05	<i>a</i>	<i>a</i>	$-10^{-3.90 \pm 0.03}$	-0.66 ± 0.05

^aIn the presence of H₂S, the uncertainties in the desorption pre-exponents and activation barriers for all three catalysts are larger than the mean values, which are therefore not included in the table.

Figure 2) dilution of the feed gas with Ar significantly reduces HD production; this response is characteristic of H₂-D₂ exchange limited by *dissociative adsorption*. Thus, one important effect of H₂S addition is to change the rate limiting step of the H₂-D₂ exchange reaction on Pd from desorption to adsorption.

The kinetic parameters of the H₂-D₂ exchange reaction over Pd₄S in the presence of H₂S were estimated by fitting the microkinetic model as expressed in eq 1 to the results of the exchange experiments. A numerical solver was used to minimize the error between the modeled and the experimental HD flow rates at all temperatures by adjusting six parameters: $\log(\nu_{\text{ads}})$, $\Delta E_{\text{ads}}^\ddagger$, $\log(\nu_{\text{des}})$, $\Delta E_{\text{des}}^\ddagger$, $\Delta H_{\text{H}_2\text{S}}$, and $\Delta S_{\text{H}_2\text{S}}$. The solver-optimized values of these parameters are listed in Table 2. The barrier to H₂ dissociation on the Pd₄S surface (0.58 ± 0.03 eV) is much higher than that on either β -Pd-hydride (0.3 ± 0.1 eV) or α -Pd-hydride (0.12 ± 0.04 eV). This result is consistent with the responses of HD production rate to changes in P_{H_2} , and it explains, in large part, the lower H₂-D₂ exchange activity of Pd₄S in the presence of H₂S relative to clean Pd. Lower inherent activity of the surface for H₂ dissociation is responsible for the large difference in onset temperature for exchange between clean Pd and Pd₄S in the presence of H₂S (Figure 1). The uncertainties in the kinetic parameters for desorption were larger than their mean values; therefore, we do not report them in the table. These large uncertainties indicate that the model is insensitive to the parameters associated with H₂ desorption and is further evidence of an adsorption-limited reaction.

Using the solver-optimized values for the kinetics parameters for H₂-D₂ exchange on Pd₄S, HD flow rates were calculated with eq 1 and are shown as solid lines in Figures 1 and 2. The model fits the data well and accurately captures the trend of decreasing H₂-D₂ exchange activity with increasing H₂S concentration. The model also accurately describes the reduced HD flow rates that result from lowering the H₂ and D₂ partial pressures by diluting the feed gas with Ar (Figure 2b).

The model also allows estimation of the coverages of H, θ_{H} (eq A10), and H₂S, $\theta_{\text{H}_2\text{S}}$ (eq 4), during H₂-D₂ exchange. Over all temperatures and H₂S concentrations, θ_{H} is negligible (<0.005), as expected for adsorption limited exchange. The values of $\theta_{\text{H}_2\text{S}}$ are plotted in Figure 3 for each H₂S concentration as a function of reaction temperature range. At low temperatures, $\theta_{\text{H}_2\text{S}}$ on the Pd₄S surface varies from ~0.5 at the lowest H₂S concentration (100 ppm) to ~0.95 at the highest H₂S concentration (2000 ppm). As the temperature increases, $\theta_{\text{H}_2\text{S}}$ decreases to ~0.05 at the lowest H₂S concentration (100 ppm) and ~0.4 at the highest H₂S

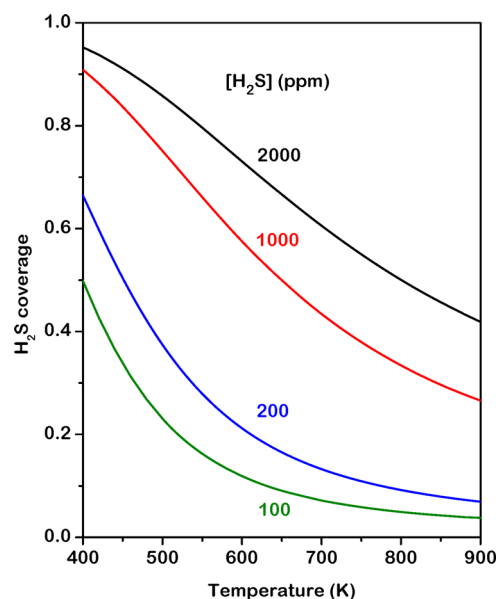


Figure 3. H₂S coverage during H₂-D₂ exchange over Pd₄S with 100, 200, 1000, and 2000 ppm H₂S and with 9 mL/min each of H₂ and D₂ in the feed gas. H₂S coverage was calculated with eq 4 and the solver-optimized values for ν_{ads} , $\Delta E_{\text{ads}}^\ddagger$, ν_{des} , $\Delta E_{\text{des}}^\ddagger$, $\Delta H_{\text{H}_2\text{S}}$, and $\Delta S_{\text{H}_2\text{S}}$. The H₂S coverage is high at low temperatures and decreases with increasing temperature and with decreasing H₂S concentration.

concentration (2000 ppm). Thus, site blocking by adsorbed H₂S also contributes to suppression of H₂-D₂ exchange activity; it is responsible for the differences among HD production rates at the different (nonzero) H₂S concentrations (Figure 1).

4.2. H₂-D₂ Exchange over Pd₇₀Cu₃₀ in the Presence of H₂S. H₂-D₂ exchange over Pd₇₀Cu₃₀ was performed in a manner similar to the Pd₄S experiments. Figure 4a–c shows the HD flow rates exiting the Pd₇₀Cu₃₀ catalyst bed at the same three H₂/D₂/Ar flow rate combinations and with the same H₂S concentrations used for Pd₄S. For comparison, Figure 4 also displays the HD flow rates measured previously exiting a clean Pd₇₀Cu₃₀ foil catalyst bed with 0 ppm H₂S in the feed gas.¹⁸ For all H₂/D₂/Ar flow rate combinations, the onset of H₂-D₂ exchange in the presence of 100 ppm H₂S occurs at ~250 K higher than the onset over the clean Pd₇₀Cu₃₀ surface with 0 ppm H₂S in the feed gas. As was the case for Pd₄S, increasing the H₂S concentration in the feed gas from 100 through 2000 ppm causes further decreases in H₂-D₂ exchange rates.

We reported previously that, on the clean Pd₇₀Cu₃₀ catalyst in the absence of H₂S, the rate of H₂-D₂ exchange is limited by

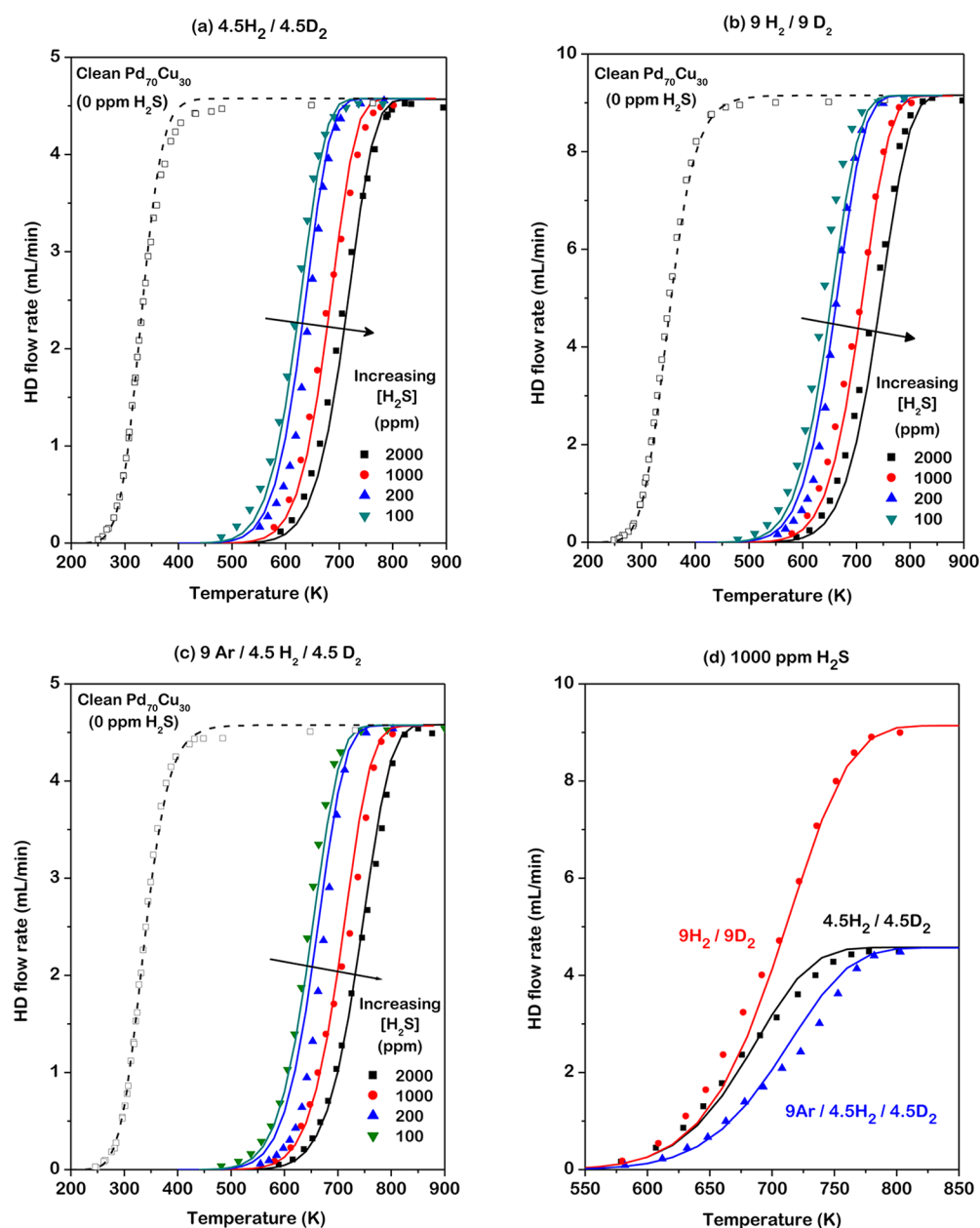


Figure 4. HD flow rates exiting a $\text{Pd}_{70}\text{Cu}_{30}$ catalyst bed with (a) 4.5 mL/min each of H_2 and D_2 in the feed gas, (b) 9 mL/min each of H_2 and D_2 in the feed gas, and (c) 9 mL/min of Ar with 4.5 mL/min each of H_2 and D_2 in the feed gas. The solid lines are fits of the microkinetic model for H_2 - D_2 exchange to the data. H_2S concentrations in the feed gas are 0, 100, 200, 1000, and 2000 ppm. Increasing the H_2S concentration in the feed gas decreases the rate of H_2 - D_2 exchange over $\text{Pd}_{70}\text{Cu}_{30}$ with all three $\text{H}_2/\text{D}_2/\text{Ar}$ feed gas combinations. (d) HD flow rates exiting the $\text{Pd}_{70}\text{Cu}_{30}$ foil catalyst bed with 1000 ppm H_2S in the feed gas, and with 9 mL/min of H_2 and D_2 ($9\text{H}_2/9\text{D}_2$), 4.5 mL/min of H_2 and D_2 ($4.5\text{H}_2/4.5\text{D}_2$), and 4.5 mL/min of H_2 and D_2 diluted with 9 mL/min of Ar. The HD flow rate exiting the $\text{Pd}_{70}\text{Cu}_{30}$ catalyst bed in the presence of 1000 ppm H_2S is significantly reduced by diluting the feed gas with Ar, indicating adsorption-limited H_2 - D_2 exchange.

the rate of recombinative H-D *desorption* due to the low barrier to H_2 dissociative adsorption.¹⁸ Figure 4d shows that the flow rate of HD product in the presence of 1000 ppm H_2S is significantly reduced when the $4.5\text{H}_2/4.5\text{D}_2$ feed gas is diluted with Ar to reduce P_{H_2} ; as noted earlier, this response is characteristic of H_2 - D_2 exchange limited by dissociative *adsorption*. Ar dilution of the feed gas with 100, 200, and 2000 ppm H_2S also reduced the rate of H_2 - D_2 exchange (results not shown in Figure 4). These results illustrate that, as was the case for Pd_4S , H_2S switches the rate-limiting step for H_2 - D_2 exchange over $\text{Pd}_{70}\text{Cu}_{30}$ from recombinative *desorption* to dissociative *adsorption*.

The kinetic parameters of the H_2 - D_2 exchange reaction over $\text{Pd}_{70}\text{Cu}_{30}$ in the presence of H_2S were estimated by fitting the microkinetic model, eq 1, to the results of the exchange experiments. Modeled HD flow rates calculated with the solver-optimized parameters (Table 2) are shown as the solid curves in Figure 4. The model accurately describes the decreasing H_2 - D_2 exchange activity with increasing H_2S concentration (Figure 4a–c) and the reduced rate of H_2 - D_2 exchange resulting from Ar dilution (Figure 4d). The intrinsic barrier to H_2 dissociation on $\text{Pd}_{70}\text{Cu}_{30}$ is much higher in the presence of H_2S (0.84 ± 0.06 eV) than on the clean $\text{Pd}_{70}\text{Cu}_{30}$ surface without H_2S in the feed gas (0.09 ± 0.02 eV). A high dissociative adsorption

barrier is consistent with the results of the Ar dilution experiments and explains, to a large extent, the lower H₂-D₂ exchange activity of Pd₇₀Cu₃₀ in the presence of H₂S than in the absence of H₂S. Lower inherent surface activity is responsible for the large increase in the onset temperature for exchange activity that occurs when H₂S is added to the reactant gas mixture (Figure 4).

Using the solver-optimized parameters, the H₂S coverage, $\theta_{\text{H}_2\text{S}}$, was calculated with eq 4 over the temperature range of the H₂-D₂ exchange reaction and with H₂S concentrations of 100, 200, 1000, and 2000 ppm (see Figure 5). At 400 K, the H₂S

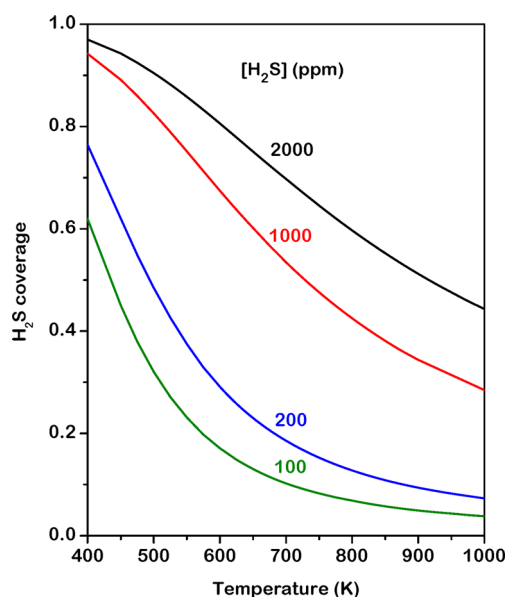


Figure 5. H₂S coverage during H₂-D₂ exchange over Pd₇₀Cu₃₀ with 100, 200, 1000, and 2000 ppm H₂S and with 9 mL/min each of H₂ and D₂ in the feed gas. H₂S coverage was calculated with eq 4 and the solver-optimized values for ν_{ads} , $\Delta E_{\text{ads}}^\ddagger$, ν_{des} , $\Delta E_{\text{des}}^\ddagger$, $\Delta H_{\text{H}_2\text{S}}$, and $\Delta S_{\text{H}_2\text{S}}$. The H₂S coverage is high at low temperatures and decreases with increasing temperature and with decreasing H₂S concentration.

coverage varies from ~ 0.6 at the lowest H₂S concentration (100 ppm) to ~ 0.95 at the highest H₂S concentration (2000 ppm). As the temperature increases, the H₂S coverage decreases to ~ 0.05 at 100 ppm H₂S and ~ 0.45 at 2000 ppm H₂S. Site blocking provides a second contribution to reduced exchange activity in the presence of H₂S; it is responsible for differences in HD production rate among the (nonzero) H₂S concentrations.

4.3. H₂-D₂ Exchange over Pd₄₇Cu₅₃ in the Presence of H₂S. H₂-D₂ exchange over Pd₄₇Cu₅₃ is influenced by the complex crystal structure of Pd₄₇Cu₅₃, which is face-centered-cubic (FCC) at temperatures above ~ 800 K, and B2 at temperatures below ~ 700 K.^{9,27,28} In the range 700–800 K, the B2 and FCC phases coexist in a two phase region. We previously reported that, in the absence of H₂S, the H₂-D₂ exchange activities of the B2 and FCC phases of Pd₄₇Cu₅₃ are significantly different.¹⁸ Here, we show that the H₂-D₂ exchange activities of B2 and FCC Pd₄₇Cu₅₃ may also differ in the presence of H₂S. Figure 6 shows the HD flow rates exiting the Pd₄₇Cu₅₃ foil catalyst bed at the same three H₂/D₂/Ar flow rate combinations and with the same H₂S concentrations as used for Pd₄S and Pd₇₀Cu₃₀. For comparison, the HD flow rates exiting a clean Pd₄₇Cu₅₃ foil catalyst bed with a B2 crystal structure and

with 0 ppm H₂S in the feed gas, reproduced from our previous work, are also shown in Figure 6.¹⁸ With 1000 and 2000 ppm H₂S in the feed gas, there is a noticeable discontinuity in the HD flow rate near 800 K. This discontinuity is likely due to a change in the intrinsic H₂-D₂ exchange activity that accompanies the change from a mixed B2/FCC phase to FCC at ~ 800 K.

When 100 ppm H₂S is added to the feed gas, the onset of H₂-D₂ exchange is ~ 300 K higher than on the clean B2 Pd₄₇Cu₅₃ catalyst without H₂S in the feed gas. Increasing the H₂S concentration in the feed gas from 100 to 2000 ppm results in small incremental reductions in the rate of H₂-D₂ exchange. On the clean B2 Pd₄₇Cu₅₃ in the absence of H₂S, the rate of H₂-D₂ exchange is desorption-limited due to the small barrier to H₂ dissociation (0.15 ± 0.02 eV).¹⁸ In the presence of 1000 ppm H₂S, however, the HD flow rate is significantly reduced when P_{H_2} is lowered by diluting the feed gas with Ar (Figure 6d) indicating adsorption-limited H₂-D₂ exchange. These results illustrate that introduction of H₂S switches the rate-limiting step of H₂-D₂ exchange over Pd₄₇Cu₅₃ from recombinative desorption to dissociative adsorption.

To estimate the kinetic parameters of H₂-D₂ exchange over Pd₄₇Cu₅₃ in the presence of H₂S, only the data below the temperature of the mixed B2/FCC to FCC phase transition (~ 800 K) was used in the solver optimization. Table 2 lists the values of the solver-optimized parameters for H₂-D₂ exchange over Pd₄₇Cu₅₃ in the presence of H₂S as well as for clean B2 Pd₄₇Cu₅₃ in the absence of H₂S.¹⁸ Using the solver-optimized values, HD flow rates were calculated with the H₂-D₂ exchange model, eq 1, and are plotted as the solid curves in Figure 6. The model accurately describes the decreasing H₂-D₂ exchange activity with increasing H₂S concentration as well as the effect of Ar dilution on the HD flow rate exiting the Pd₄₇Cu₅₃. Our model indicates that the barrier to H₂ dissociation on the sulfur-poisoned Pd₄₇Cu₅₃ catalyst (0.46 ± 0.05 eV) is much higher than on the clean Pd₄₇Cu₅₃ catalyst (0.15 ± 0.02 eV) in the absence of H₂S. This difference in inherent activity is responsible for the large increase in the onset temperature for H₂-D₂ exchange when as little as 100 ppm of H₂S is added to the reactant gas mixture.

The H₂S coverage, $\theta_{\text{H}_2\text{S}}$, was also calculated with the solver-optimized parameters and eq 4 as a function of temperature and H₂S concentration and is plotted in Figure 7. At ~ 500 K, the H₂S coverage on Pd₄₇Cu₅₃ is greater than 0.9 for all four H₂S concentrations. As the temperature increases, the H₂S coverage decreases rapidly until the coverage is less than 0.2 for all four H₂S concentrations at 1000 K. Site blocking by H₂S is responsible for the small differences among HD production rates measured at different (nonzero) H₂S concentrations.

4.4. Comparison of H₂-D₂ Exchange over Pd₄S, Pd₇₀Cu₃₀, and Pd₄₇Cu₅₃. The effect of H₂S on the rate of H₂-D₂ exchange over Pd₄S, Pd₇₀Cu₃₀, and Pd₄₇Cu₅₃ was similar for all three catalysts: 100 ppm of H₂S significantly reduced the rate of H₂-D₂ exchange relative to that over the clean surfaces in the absence of H₂S, and the rate of H₂-D₂ exchange decreased with increasing H₂S concentration in the feed gas. Figure 8 shows a comparison of the HD flow rates exiting the Pd₄S, Pd₇₀Cu₃₀, and Pd₄₇Cu₅₃ foil catalyst beds with 1000 ppm H₂S and with 9 mL/min each of H₂ and D₂ in the feed gas. At each H₂S concentration (100–2000 ppm H₂S), the trend in the H₂-D₂ exchange rate followed that observed at 1000 ppm H₂S: the H₂-D₂ exchange activity decreased in the order Pd₄S > Pd₇₀Cu₃₀ > Pd₄₇Cu₅₃.

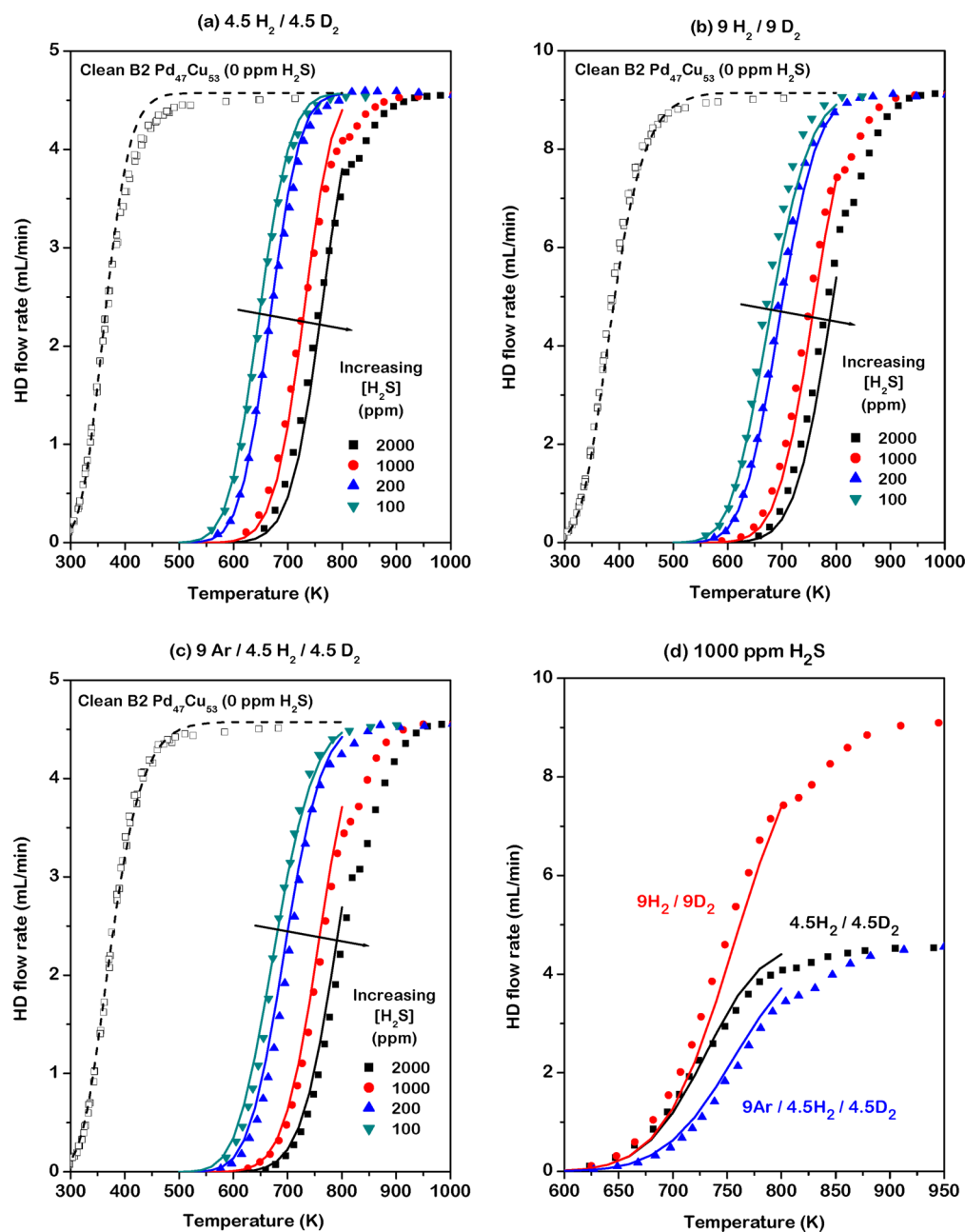


Figure 6. HD flow rates exiting a $\text{Pd}_{47}\text{Cu}_{53}$ catalyst bed with (a) 4.5 mL/min each of H_2 and D_2 in the feed gas, (b) 9 mL/min each of H_2 and D_2 in the feed gas, and (c) 9 mL/min of Ar with 4.5 mL/min each of H_2 and D_2 in the feed gas. The solid lines are fits of the microkinetic model for H_2 - D_2 exchange to the data. H_2S concentrations in the feed gas are 0, 100, 200, 1000, and 2000 ppm. Increasing the H_2S concentration in the feed gas decreases the rate of H_2 - D_2 exchange over $\text{Pd}_{47}\text{Cu}_{53}$ with all three $\text{H}_2/\text{D}_2/\text{Ar}$ feed gas combinations. (d) HD flow rates exiting the $\text{Pd}_{47}\text{Cu}_{53}$ catalyst bed with 1000 ppm H_2S in the feed gas, and with three different $\text{H}_2/\text{D}_2/\text{Ar}$ feed gas combinations: 9 mL/min of H_2 and D_2 ($9\text{H}_2/9\text{D}_2$), 4.5 mL/min of H_2 and D_2 ($4.5\text{H}_2/4.5\text{D}_2$), and 4.5 mL/min of H_2 and D_2 diluted with 9 mL/min of Ar ($9\text{Ar}/4.5\text{H}_2/4.5\text{D}_2$). Diluting the $4.5\text{H}_2/4.5\text{D}_2$ feed gas with Ar ($9\text{Ar}/4.5\text{H}_2/4.5\text{D}_2$) significantly reduces the HD flow rate, indicating adsorption-limited H_2 - D_2 exchange. Only data below 800 K were used in our solver optimization and therefore the fit of the model to the data is only shown below 800 K.

H_2S reduces the rate of H_2 - D_2 exchange over all three catalysts by two distinct mechanisms. First, in the presence of H_2S , activation barriers to the dissociative adsorption of H_2 are significantly higher than the corresponding barriers on clean surfaces in the absence of H_2S . These differences are highlighted in Figure 9, which compares potential energy diagrams for H_2 dissociation over Pd_4S , $\text{Pd}_{70}\text{Cu}_{30}(\text{H}_2\text{S})$, and $\text{Pd}_{47}\text{Cu}_{53}(\text{H}_2\text{S})$ to those for H_2 dissociation over clean α -Pd-hydride, β -Pd-hydride, $\text{Pd}_{70}\text{Cu}_{30}$, and B2 $\text{Pd}_{47}\text{Cu}_{53}$ in the absence of H_2S .¹⁸ Differences among the adsorption barriers

and adsorption pre-exponentials (Table 2) for H_2 - D_2 exchange in the presence of H_2S on the three surfaces certainly reflect differences in local structure and chemistry of the surfaces. While we did not perform detailed characterization of the H_2S -exposed surfaces as part of this work, we note that the literature suggests that the chemistries of the three terminating surfaces are likely to be different. Both Pd_4S and a mixed PdCu sulfide, $\text{Pd}_{13}\text{Cu}_3\text{S}_7$, have been identified as components of a thin (~ 5 μm) surface layer that forms on $\text{Pd}_{70}\text{Cu}_{30}$ upon exposure to H_2S at 623 K; $\text{Pd}_{47}\text{Cu}_{53}$ exposed to H_2S at 723 K is terminated

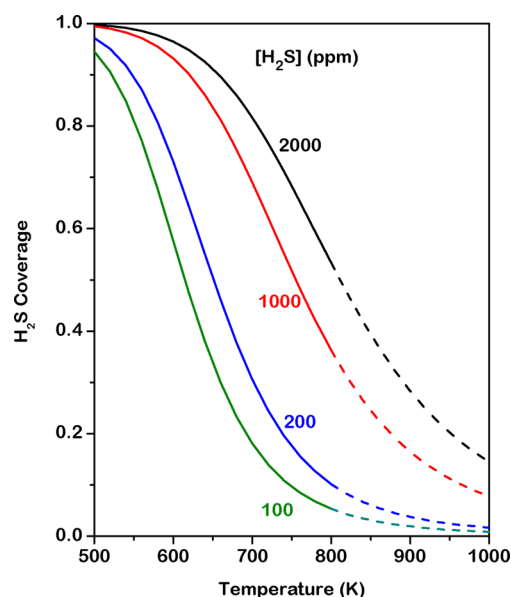


Figure 7. H₂S coverage during H₂-D₂ exchange over Pd₄₇Cu₅₃ with 100, 200, 1000, and 2000 ppm H₂S and with 9 mL/min each of H₂ and D₂ in the feed gas. H₂S coverage was calculated with eq 4 and the solver-optimized values for ν_{ads} , $\Delta E_{\text{ads}}^{\ddagger}$, ν_{des} , $\Delta E_{\text{des}}^{\ddagger}$, $\Delta H_{\text{H}_2\text{S}}$, and $\Delta S_{\text{H}_2\text{S}}$. The H₂S coverage is high at low temperatures and decreases with increasing temperature and with decreasing H₂S concentration. A dashed line is shown for temperatures above 800 K because only data below 800 K was used in our solver optimization.

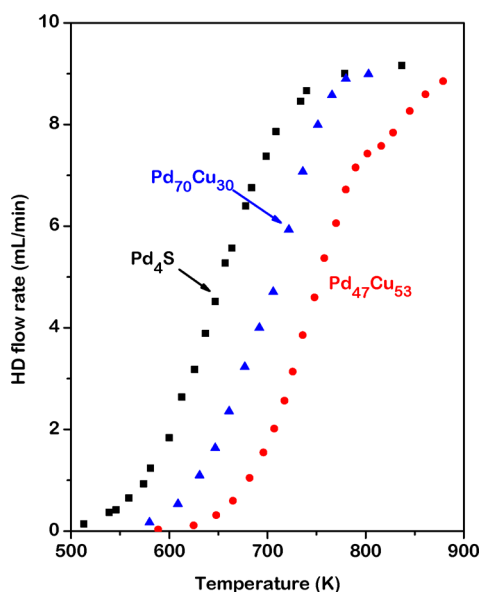


Figure 8. Comparison of the HD flow rates exiting Pd₄S, Pd₇₀Cu₃₀, and Pd₄₇Cu₅₃ foil catalyst beds with 1000 ppm H₂S and 9 mL/min of H₂ and D₂ in the feed gas. The rate of HD production over Pd₄S is the highest followed by Pd₇₀Cu₃₀ and Pd₄₇Cu₅₃.

by an even thinner ($\sim 1 \mu\text{m}$) layer that contains only the mixed Pd₁₃Cu₃S₇ sulfide.¹⁰

The second effect of H₂S on H₂-D₂ exchange rates is that it blocks a fraction of the high barrier, low activity dissociation sites. Figure 10 compares model-calculated H₂S coverages on Pd₄S, Pd₇₀Cu₃₀, and Pd₄₇Cu₅₃ during H₂-D₂ exchange in the presence of 1000 ppm H₂S and 9 mL/min each of H₂ and D₂. At low temperature (500 K), the H₂S coverage is greater than

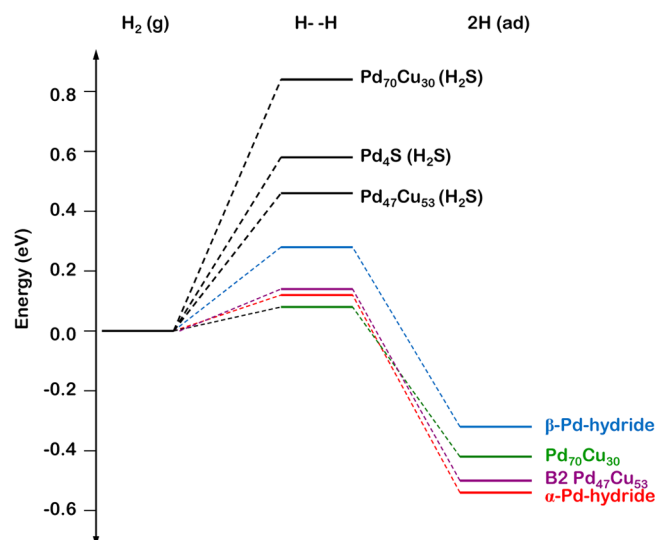


Figure 9. Potential energy diagrams for H₂ dissociation on Pd₇₀Cu₃₀, Pd₄S, and Pd₄₇Cu₅₃ in the presence of H₂S, and for clean β -Pd-hydride, α -Pd-hydride, Pd₇₀Cu₃₀, and B2 Pd₄₇Cu₅₃.

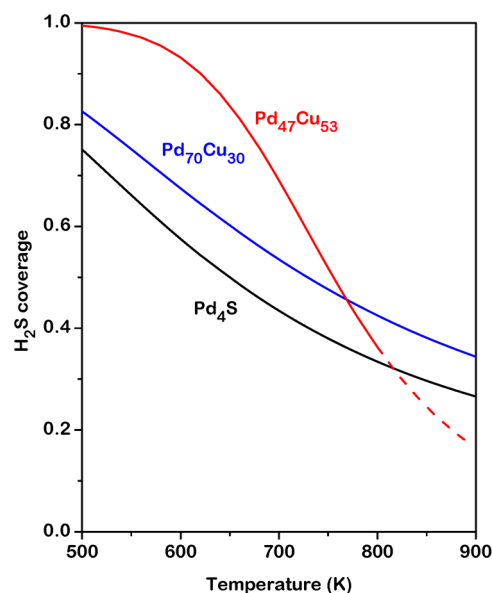


Figure 10. H₂S coverage on Pd₄S, Pd₇₀Cu₃₀, and Pd₄₇Cu₅₃ during H₂-D₂ exchange with 1000 ppm H₂S and 9 mL/min each of H₂ and D₂ in the feed gas. H₂S coverage was calculated with eq 4 and the solver-optimized parameters listed in Table 2.

0.7 for all three catalysts and increases in the order: Pd₄S < Pd₇₀Cu₃₀ < Pd₄₇Cu₅₃. As the temperature increases, the H₂S coverage decreases for all three catalysts. The rate of change in H₂S coverage with increasing temperature is similar for Pd₄S and Pd₇₀Cu₃₀, but the H₂S coverage decreases much more quickly on the Pd₄₇Cu₅₃ surface. At 900 K, the H₂S coverage is lowest on Pd₄₇Cu₅₃ (0.16), followed by Pd₄S (0.27) and Pd₇₀Cu₃₀ (0.34).

Differences in H₂S coverage among the three surfaces are reflected in the thermodynamic parameters for H₂S adsorption (Table 2). Pd₄S and Pd₇₀Cu₃₀(H₂S) display identical values of $\Delta H_{\text{H}_2\text{S}}$ (-0.21 eV) and $\Delta S_{\text{H}_2\text{S}}$ ($-10^{-3.15} \text{ eV/K}$). This value of $\Delta H_{\text{H}_2\text{S}}$ is in the range of those observed for nondissociative H₂S adsorption on relatively inert surfaces, such as carbons,²⁹ suggesting that H₂S is not strongly bound to the surface sulfide.

$\Delta S_{\text{H}_2\text{S}}$ compares well with an estimate from statistical mechanics for a case of molecular adsorption/desorption with a mobile transition state: -10^{-3} eV/K.³⁰ With $\Delta H_{\text{H}_2\text{S}} \sim -0.66$ eV, H_2S interacts more strongly with the $\text{Pd}_{47}\text{Cu}_{53}(\text{H}_2\text{S})$ surface than it does with either Pd_4S or $\text{Pd}_{70}\text{Cu}_{30}(\text{H}_2\text{S})$. While the atomic level reasons for this difference are not clear, we note that Pd_4S appears at the surfaces of both Pd_4S and $\text{Pd}_{70}\text{Cu}_{30}(\text{H}_2\text{S})$, but not $\text{Pd}_{47}\text{Cu}_{53}(\text{H}_2\text{S})$, and could, therefore, be responsible for the common H_2S adsorption behavior of Pd_4S and $\text{Pd}_{70}\text{Cu}_{30}(\text{H}_2\text{S})$.

5. CONCLUSIONS

We have investigated the effect of H_2S on H_2 dissociation over Pd_4S , $\text{Pd}_{70}\text{Cu}_{30}$, and $\text{Pd}_{47}\text{Cu}_{53}$ surfaces by microkinetic analysis of the H_2 - D_2 exchange reaction in the presence of varying concentrations of H_2S . For all three catalysts, the H_2 - D_2 exchange activity is significantly lower in the presence of H_2S than that on the clean surfaces in the absence of H_2S , and the rate of H_2 - D_2 exchange decreases with increasing H_2S concentration. Microkinetic analysis indicates that H_2S suppresses the rate of H_2 - D_2 exchange by two mechanisms. H_2S reduces the inherent activity of the surface, which is reflected in an increase of the barrier to H_2 dissociative adsorption. H_2S also adsorbs onto the surfaces and blocks some of the dissociation sites. H_2S coverage, and the extent of site blocking that it causes, depends on both the alloy surface and the conditions of exposure (T , $P_{\text{H}_2\text{S}}$).

■ APPENDIX: DERIVATION OF THE H_2 - D_2 EXCHANGE MODEL

The integral mass balance on HD is

$$\int_0^{F_{\text{HD,out}}} \frac{dF_{\text{HD}}}{r_{\text{HD}}} = A \quad (\text{A1})$$

where dF_{HD} is the differential HD flow rate, $F_{\text{HD,out}}$ is the HD flow rate exiting the catalyst bed, A is the catalyst surface area, and r_{HD} is the HD production rate.³¹ The HD production rate, r_{HD} , is given by the microkinetic expression:

$$r_{\text{HD}} = 2k_{\text{des}}\theta_{\text{H}}\theta_{\text{D}} - k_{\text{ads}}P_{\text{HD}}\theta_*^2 \quad (\text{A2})$$

where k_{des} is the HD desorption rate constant, θ_{H} is the coverage of H atoms, θ_{D} is the coverage of D atoms, k_{ads} is the HD adsorption rate constant, P_{HD} is the HD partial pressure, and θ_* is the fraction of surface sites that are available for adsorption:

$$\theta_* = 1 - \theta_{\text{H}_2\text{S}} - \theta_{\text{H}} - \theta_{\text{D}} \quad (\text{A3})$$

where $\theta_{\text{H}_2\text{S}}$ is the H_2S coverage. Because we are assuming that isotopic effects are negligible, and the partial pressures of H_2 and D_2 are equal for all experiments, the coverages of H (θ_{H}) and D (θ_{D}) atoms are each assumed to be equal to one-half of the total coverage of H and D atoms ($\theta_{\text{H+D}}$):

$$\theta_{\text{H}} = \theta_{\text{D}} = \frac{\theta_{\text{H+D}}}{2}$$

Therefore, the microkinetic expression for the rate of HD production (r_{HD}), eq A2, becomes:

$$r_{\text{HD}} = \frac{1}{2}k_{\text{des}}\theta_{\text{H+D}}^2 - k_{\text{ads}}P_{\text{HD}}\theta_*^2 \quad (\text{A4})$$

To substitute the microkinetic expression for the rate of HD production, eq A4, into the mass balance on HD, eq A1, the

HD partial pressure in eq A4 must be converted into HD flow rate, F_{HD} :

$$r_{\text{HD}} = \frac{1}{2}k_{\text{des}}\theta_{\text{H+D}}^2 - \frac{k_{\text{ads}}F_{\text{HD}}P_{\text{total}}\theta_*^2}{F_{\text{total}}} \quad (\text{A5})$$

where

$$F_{\text{HD}} = \frac{F_{\text{total}}P_{\text{HD}}}{P_{\text{total}}}$$

and P_{total} is the total pressure and F_{total} is the total flow rate of all gases. Substituting the HD production rate, eq A5, into the integral mass balance on HD, eq A1, gives

$$\int_0^{F_{\text{HD,out}}} \frac{dF_{\text{HD}}}{\frac{1}{2}k_{\text{des}}\theta_{\text{H+D}}^2 - \frac{k_{\text{ads}}F_{\text{HD}}P_{\text{total}}\theta_*^2}{F_{\text{total}}}} = A \quad (\text{A6})$$

Integrating eq A6 and solving for the flow rate of HD exiting the catalyst bed gives:

$$F_{\text{HD,out}} = \frac{k_{\text{des}}\theta_{\text{H+D}}^2 F_{\text{total}}}{2k_{\text{ads}}P_{\text{total}}\theta_*^2} \left[1 - \exp\left(\frac{-k_{\text{ads}}P_{\text{total}}A\theta_*^2}{F_{\text{total}}}\right) \right] \quad (\text{A7})$$

At steady-state, the changes in the coverages of H_2S ($\theta_{\text{H}_2\text{S}}$), H (θ_{H}), and D (θ_{D}) are zero:

$$\frac{d\theta_{\text{H}_2\text{S}}}{dt} = \frac{d\theta_{\text{H}}}{dt} = \frac{d\theta_{\text{D}}}{dt} = 0$$

Starting with an atomic balance on H gives:

$$\begin{aligned} \frac{d\theta_{\text{H}}}{dt} &= 0 \\ &= 2k_{\text{ads}}P_{\text{H}_2}\theta_*^2 + k_{\text{ads}}P_{\text{HD}}\theta_*^2 - 2k_{\text{des}}\theta_{\text{H}}^2 - 2k_{\text{des}}\theta_{\text{H}}\theta_{\text{D}} \end{aligned}$$

where P_{H_2} is the H_2 partial pressure and P_{HD} is the HD partial pressure. Assuming that the coverage of H and D atoms is equal to one-half of the total coverage of H and D, the change in the coverage of H atoms is given by

$$\frac{d\theta_{\text{H}}}{dt} = 0 = 2k_{\text{ads}}P_{\text{H}_2}\theta_*^2 + k_{\text{ads}}P_{\text{HD}}\theta_*^2 - k_{\text{des}}\theta_{\text{H+D}}^2 \quad (\text{A8})$$

The partial pressure of H_2 and the partial pressure of HD are related to the partial pressure of H_2 in the feed gas ($P_{\text{H}_2,\text{feed}}$) by the stoichiometry of the H_2 - D_2 exchange reaction:

$$P_{\text{H}_2} = P_{\text{H}_2,\text{feed}} - \frac{1}{2}P_{\text{HD}} \quad (\text{A9})$$

Substituting eq A9 into eq A8, and solving gives the total coverage of H and D atoms at steady-state ($\theta_{\text{H+D}}$):

$$\theta_{\text{H+D}} = \sqrt{2 \frac{k_{\text{ads}}P_{\text{H}_2,\text{feed}}\theta_*^2}{k_{\text{des}}}} \quad (\text{A10})$$

A balance on H_2S gives

$$\frac{d\theta_{\text{H}_2\text{S}}}{dt} = 0 = k_1P_{\text{H}_2\text{S}}\theta_* - k_{-1}\theta_{\text{H}_2\text{S}}$$

where k_1 is the H_2S adsorption rate constant and k_{-1} is the H_2S desorption rate constant. Solving for $\theta_{\text{H}_2\text{S}}$ gives

$$\theta_{\text{H}_2\text{S}} = K_{\text{H}_2\text{S}}P_{\text{H}_2\text{S}}\theta_* \quad (\text{A11})$$

where $K_{\text{H}_2\text{S}}$ is the H_2S adsorption/desorption equilibrium constant that is given by

$$K_{\text{H}_2\text{S}} = \frac{k_1}{k_{-1}} = \exp\left(\frac{\Delta S_{\text{H}_2\text{S}}}{k_B}\right) \exp\left(\frac{-\Delta H_{\text{H}_2\text{S}}}{k_B T}\right)$$

Now, substituting $\theta_{\text{H}_2\text{S}}$, eq A11, $\theta_{\text{H}+\text{D}}$, eq A10 into the expression for the fraction of the surface sites available for adsorption θ_* , eq A3, gives

$$\theta_* = 1 - K_{\text{H}_2\text{S}} P_{\text{H}_2\text{S}} \theta_* - \sqrt{2 \frac{k_{\text{ads}}}{k_{\text{des}}} P_{\text{H}_2, \text{feed}} \theta_*}$$

Solving for θ_* gives

$$\theta_* = \left(1 + K_{\text{H}_2\text{S}} P_{\text{H}_2\text{S}} + \sqrt{2 \frac{k_{\text{ads}}}{k_{\text{des}}} P_{\text{H}_2, \text{feed}}} \right)^{-1} \quad (\text{A12})$$

Substituting θ_* , eq A12, and $\theta_{\text{H}+\text{D}}$, eq A10, into eq A7 gives the $\text{H}_2\text{-D}_2$ exchange model:

$$F_{\text{HD}, \text{out}} = F_{\text{H}_2, \text{feed}} \left[1 - \exp\left\{ \left(-k_{\text{ads}} P_{\text{total}} A \right) \left(F_{\text{total}} \left(1 + K_{\text{H}_2\text{S}} P_{\text{H}_2\text{S}} + \sqrt{2 \frac{k_{\text{ads}}}{k_{\text{des}}} P_{\text{H}_2, \text{feed}}} \right)^2 \right) \right\} \right]$$

where

$$F_{\text{H}_2, \text{feed}} = \frac{F_{\text{total}} P_{\text{H}_2, \text{feed}}}{P_{\text{total}}}$$

AUTHOR INFORMATION

Corresponding Author

*E-mail: jbmiller@andrew.cmu.edu. Phone: 412-268-9517.

Notes

The authors declare no competing financial interest.

ACKNOWLEDGMENTS

As part of the National Energy Technology Laboratory's Regional University Alliance (NETL-RUA), a collaborative initiative of the NETL, this technical effort was performed under the RES contract DE-FE0004000.

REFERENCES

- (1) Stiegel, G. J.; Ramezan, M. *Int. J. Coal Geol.* **2006**, *65*, 173.
- (2) Balovnev, Y. *Russ. J. Phys. Chem.* **1974**, *48*, 409.
- (3) Davis, W. D. *Diffusion of Gases through Palladium*; U.S. Atomic Energy Commission: Washington, DC, 1954.
- (4) Gorman, J. K.; Nardella, W. R. *Vacuum* **1962**, *12*, 19.
- (5) Morreale, B. D.; Ciocco, M. V.; Enick, R. M.; Morsi, B. I.; Howard, B. H.; Cugini, A. V.; Rothenberger, K. S. *J. Membr. Sci.* **2003**, *212*, 87.
- (6) Iyoha, O. University of Pittsburgh, 2007.
- (7) Iyoha, O.; Enick, R.; Killmeyer, R.; Morreale, B. *J. Membr. Sci.* **2007**, *305*, 77.
- (8) Iyoha, O.; Enick, R. M.; Killmeyer, R. P.; Howard, B. H.; Ciocco, M. V.; Morreale, B. D. *J. Membr. Sci.* **2007**, *306*, 103.
- (9) Kulprathipanja, A.; Alptekin, G. O.; Falconer, J. L.; Way, J. D. *J. Membr. Sci.* **2005**, *254*, 49.
- (10) Morreale, B. D. University of Pittsburgh, 2006.
- (11) Morreale, B. D.; Ciocco, M. V.; Howard, B. H.; Killmeyer, R. P.; Cugini, A.; Enick, R. M. *J. Membr. Sci.* **2004**, *241*, 219.

(12) Morreale, B. D.; Howard, B. H.; Iyoha, O. U.; Enick, R. M.; Ling, C.; Sholl, D. S. *Ind. Eng. Chem. Res.* **2007**, *46*, 6313.

(13) O'Brien, C. P.; Gellman, A. J.; Morreale, B. D.; Miller, J. B. *J. Membr. Sci.* **2011**, *371*, 263.

(14) O'Brien, C. P.; Howard, B. H.; Miller, J. B.; Morreale, B. D.; Gellman, A. J. *J. Membr. Sci.* **2010**, *349*, 380.

(15) Hurlbert, R. C.; Konecny, J. O. *J. Chem. Phys.* **1961**, *34*, 655.

(16) Katsusa, H.; Farraro, R. J.; McLellan, R. B. *Acta Metall.* **1979**, *27*, 1111.

(17) Ledentu, V.; Dong, W.; Sautet, P. *Surf. Sci.* **1998**, *412–413*, 518.

(18) O'Brien, C. P.; Miller, J. B.; Morreale, B. D.; Gellman, A. J. *J. Phys. Chem. C* **2011**, *115*, 24221.

(19) Wilke, S.; Scheffler, M. *Surf. Sci.* **1995**, *329*, L605.

(20) Holleck, G. L. *J. Phys. Chem. B* **1970**, *74*, 503.

(21) Iyoha, O.; Enick, R.; Killmeyer, R.; Howard, B.; Morreale, B.; Ciocco, M. *J. Membr. Sci.* **2007**, *298*, 14.

(22) Yang, J. Y.; Nishimura, C.; Komaki, M. *J. Alloys Compd.* **2007**, *446–447*, 575.

(23) Yang, J. Y.; Nishimura, C.; Komaki, M. *J. Membr. Sci.* **2008**, *309*, 246.

(24) Miller, J. B.; Matranga, C.; Gellman, A. J. *Surf. Sci.* **2008**, *602*, 375.

(25) Kamakoti, P.; Morreale, B. D.; Ciocco, M. V.; Howard, B. H.; Killmeyer, R. P.; Cugini, A. V.; Sholl, D. S. *Science* **2005**, *307*, 569.

(26) de Levie, R. *J. Chem. Educ.* **1999**, *76*, 1594.

(27) Howard, B. H.; Killmeyer, R. P.; Rothenberger, K. S.; Cugini, A. V.; Morreale, B. D.; Enick, R. M.; Bustamante, F. *J. Membr. Sci.* **2004**, *241*, 207.

(28) Yuan, L.; Goldbach, A.; Xu, H. *J. Phys. Chem. B* **2007**, *111*, 10952.

(29) Michalak, W. D.; Broitman, E.; Alvin, M. A.; Gellman, A. J.; Miller, J. B. *Appl. Catal. A: Gen* **2009**, *362*, 8.

(30) Dumesic, J. A.; Rudd, D. F.; Aparicio, L. M.; Rekoske, J. E.; Trevino, A. A. *The Microkinetics of Heterogeneous Catalysis*; American Chemical Society: Washington, DC, 1993.

(31) Fogler, H. S. *Elements of Chemical Reaction Engineering*; Prentice Hall International, Inc.: New York, 1999.